BMC Plant Biology

RESEARCH

Open Access

Assessment of the impact of biodegradable lignin nanoparticles encapsulating IAA on tomato development: from seed to fruit

Rodrigo Faleiro[1,8*], Magda Andreia Tessmer[2], Anderson Espirito Santo Pereira[3,4], Leonardo Fernandes Fraceto[3], Marcelle Sanches Rampasso[8], Marcela Trevenzoli Miranda[6], Maria Dolores Pissolato[5], Fábio Cassola[7], Rafael Vasconcelos Ribeiro[6] and Juliana Lischka Sampaio Mayer[8*]

Abstract

Polymeric nanoparticles have emerged as promising nanocarriers for plant growth regulators (PGRs) in agriculture, enhancing plant growth and boosting fruit and cereal yields. Among these, lignin nanoparticles (LNPs) stand out due to their biodegradability and low production cost. However, few studies have evaluated the biological effects of LNPs encapsulating PGRs — particularly their dose-dependent impacts across the entire plant life cycle. Therefore, our study aims to evaluate the efficiency of lignin nanoparticles (LNPs) encapsulating indole-3-acetic acid (IAA) compared with free application of the hormone. We employed a multidisciplinary approach to comprehensively assess the impacts of different LNPs-IAA concentrations. Germination tests and morphometric analyses were conducted, along with anatomical analyses of seeds, seedlings, and vegetative organs using light microscopy. Confocal microscopy analyses to examine LNP uptake and translocation. Additionally, leaf gas exchange parameters and photosynthetic pigment levels were measured. The lignin nanoparticles were also characterized in terms of length, polydispersity index, zeta potential and encapsulation efficiency. All variables were subjected to normality tests, variance analysis, and post-hoc tests. Structural analysis revealed that LNP application did not alter overall plant anatomy architecture, except for inducing differences in xylem area among vegetative organs. Additionally, LNPs were rapidly absorbed by seeds in less than 5 h and were transported exclusively via the apoplastic pathway. The composition of lignin nanoparticles influenced germination rates and time. Application with lower concentrations showed minimal statistical significance, whereas higher concentrations exhibited phytotoxic effects. Thus, our study highlights the critical importance of optimizing nanocarrier concentrations for plant growth enhancement, demonstrating that lignin nanoparticles (LNPs) represent a promising nanoformulation for bioactive compound encapsulation.

Keywords Crop science, Encapsulation, Plant growth regulators, Nanotechnology, Sustainability

*Correspondence:
Rodrigo Faleiro
rodsfaleiro@gmail.com
Juliana Lischka Sampaio Mayer
mayerju@unicamp.br
Full list of author information is available at the end of the article

Introduction

Nanotechnology has recently gained significant attention in agricultural science due to its potential to enhance productivity. In agriculture, it presents a promising alternative to reducing reliance on traditional pesticides and fertilizers [1–3]. Furthermore, it offers potential solutions for mitigating heavy metal contamination in soils [4, 5], as well as various biotic and abiotic stresses [6, 7]. Nanoparticles (NPs) can be synthesized from both organic and inorganic materials [8]. One of the main advantages of NPs is their high efficiency in transporting substances or molecules, attributed to their large surface area, strong adhesion properties, and rapid delivery to target sites [1]. Additionally, their ability to encapsulate different molecules enables the sustained release of active ingredients, improving their absorption by plants and, consequently, their biological effectiveness [9].

While most studies have focused on the effects of metallic nanoparticles (NPs), polymeric NPs have emerged as a promising alternative. These NPs function as efficient carriers for bioactive compounds and offer a sustainable solution due to their biodegradable and biocompatible nature. For instance, lignin nanoparticles (LNPs) have been investigated for various applications, including pharmaceuticals, biofuels, lignocellulosic materials, and nanomaterials [10, 11]. Their synthesis involves simple methods with short reaction times and minimal chemical consumption [10]. Notably, LNPs are biodegradable [6] and exhibit antioxidant and antibacterial properties due to the presence of phenolic compounds in their structure [7]. In agriculture, LNPs have demonstrated the ability to promote maize seedling growth when applied alone [12] and to enhance plant biomass when used as carriers for gibberellic acid [13].

The use of nanoparticles (NPs) encapsulating plant growth regulators (PGRs) holds significant potential for enhancing resistance to abiotic stress and promoting biomass production [14, 15]. Furthermore, nanoencapsulation is a groundbreaking tool for delivering bioactive compounds in an economically affordable and environmentally friendly manner [14, 15]. Numerous studies have demonstrated that specific polymeric nanocarriers are highly effective in this regard, with many of these studies reporting superior biological efficacy, including improvements in seed germination, plant growth, and fruit production [16–20].

PGRs are natural or synthetic compounds that significantly influence the physiology and metabolism of higher plants, particularly at low concentrations [21]. This group includes hormones and synthetic analogs, which provide benefits such as improved crop management, increased productivity, and enhanced quality and yield [21, 22]. Among the primary PGRs used in agriculture, auxins stand out due to their diverse roles in plant development and metabolism [23]. These hormones regulate key processes from embryogenesis to fruit ripening by controlling cell division, expansion, and differentiation [21, 24]. Additionally, auxins play essential roles in plant architecture, germination, and xylem development. However, the potential phytotoxic effects of high auxin concentrations, as well as their interactions with other PGRs, such as ethylene and abscisic acid (ABA), should be carefully considered, as they may negatively impact plant growth [25, 26].

Although polymeric nanoparticles, including lignin-based ones, have shown positive effects on some plant species, their efficacy as carriers for plant growth regulators (particularly auxins) and their impacts on the full plant life cycle remain underexplored. To bridge this gap, this study evaluates the efficiency of lignin nanoparticles (LNPs) in encapsulating indole- 3-acetic acid (IAA) in'Sweet Grape'cherry tomatoes (*Solanum lycopersicum* L.), comparing LNP-encapsulated IAA with its free form at equivalent concentrations. We hypothesize that LNPs act as effective nanocarriers for IAA, enhancing plant development at lower concentrations, offering a sustainable approach for phytohormone delivery in agriculture.

Materials and methods

Botanical material

The seeds of hybrid cherry tomatoes (*Solanum lycopersicum* L.),"sweet grapes,"were extracted from the fruits, air-dried at room temperature (24 °C), and then stored in microcentrifuge tubes (Eppendorf Group, Hamburg, Germany) protected from light exposure. The hybrid was chosen because of its high fruit quality and yield, as well as its ease of cultivation and shorter life cycle (120–160 days).

Preparation and characterization of LNPs

The LNPs were prepared using the antisolvent method proposed by Falsini et al. [13], with modifications. The organic phase was prepared by dissolving 6 mL of lignin (5 mg/mL) in a 70% ethanol solution under magnetic stirring in a beaker. To this solution, 0.105 mg of carvacrol and 2 mg of IAA (Sigma–Aldrich, Brazil) were added until completely dissolved. The lignin solution was then added to 30 mL of water, and the mixture was stirred for 30 min. After preparation, ethanol was removed via rotary evaporation, and the final volume was adjusted to 20 mL. For labeled nanoparticles, the fluorophore 1,2-dipalmitoyl-sn-glycero- 3-phosphoethanolamine-N-(Lissamine rhodamine B sulfonyl chloride) (0.1% of the lignin mass) was added to the organic phase.

The size distribution and polydispersity index of the nanoparticles were determined using the Dynamic Light Scattering (DLS) technique, with scattered light detected

at a 90° angle using a Zetasizer Nano ZS90 instrument (Malvern Instruments, UK). The zeta potential was measured using the same instrument via the electrophoresis method. All samples were analyzed in triplicate at 25 °C. The encapsulation efficiency and quantification of the active ingredient (IAA) were analyzed using the HPLC technique describe in supplementary Table 01.

For the release profile of IAA, in vitro release kinetics were evaluated using a two-compartment dialysis system. Nanoparticle suspensions (4 mL) were loaded into the donor compartment, separated by a 1 kDa molecular weight cutoff dialysis membrane from the acceptor compartment containing 2% pluronic solution (to enhance compound solubility). Aliquots were periodically collected from the acceptor compartment over 24 h, with released compounds quantified via HPLC. All release assays were conducted in triplicate at 25 °C, with results presented in figure supplementary 02.

Treatments

To assess the efficiency of applying lignin nanoparticles encapsulating auxin, the following treatments were used: distilled water (control), lignin nanoparticles (LNPs) at a concentration of 50 µg/ml, lignin nanoparticles with IAA encapsulation (LNPs-IAA) at concentrations of 0.05, 5, 50, and 100 µg/ml, and IAA solutions at concentrations of 0.05, 5, 50, and 100 µg/ml. IAA (Sigma–Aldrich, Brazil) was dissolved in potassium hydroxide (Sigma–Aldrich, Brazil) and distilled water, with a final volume of 100 mL.

The seeds were sanitized with a 2.5% sodium hypochlorite solution and rinsed with distilled water. The samples were then immersed in solutions of each treatment, as previously described, and agitated for 5 h. For seed treatment, 100 seeds were placed in Eppendorf tubes, with a final volume of 1 mL for each solution. Following this process, the seeds were randomly planted in 5-L pots (25 seeds per pot) containing a substrate composed of coconut fiber, carbonized rice husk, peat, and vermiculite (HL1000, Hollan Grow, Brazil). After 10 days, thinning was performed, leaving only one seedling per pot, resulting in a total of 15 seedlings per treatment. At this stage, root and hypocotyl lengths were measured in 15 replicates per treatment.

Growth conditions

The pots were fertilized with a slow-release macro- and micronutrient formulation (Basacot®), containing N (16%), P_2O_5 (8%), K_2O (12%), MgO (2%), S (5%), Fe (0.4%), B (0.02%), Zn (0.02%), Cu (0.05%), Mn (0.06%), and Mo (0.015%), following recommendations based on pot size and tomato cultivation guidelines. The fertilizer was applied around the seedlings.

Throughout the 140-day experimental period, the plants were maintained in a greenhouse under regular irrigation at 7:00, 10:00, 13:00, 16:00, and 18:00, each lasting 2 min, with a total water volume of 5,225 mL distributed across five sprinklers. The experiments were conducted between February and June, corresponding to late summer and autumn. The temperature (maximum, average, and minimum) and relative humidity (%) recorded inside the greenhouse during the experiment are presented in supplementary Fig. 01.

Germination and biometric analyses

To evaluate germination percentage and germination time, 100 seeds per treatment underwent the same sanitization and preparation process described previously. After 5 h of immersion, the seeds were placed in gerboxes lined with filter paper moistened with distilled water at a ratio of 2.5 times the mass of the dry paper. The boxes were then maintained in a growth chamber (BOD) at 25 °C. The analysis was performed in four replicates of 25 seeds per treatment over a 10-day period. Germination percentage was calculated based on the number of seeds exhibiting radicle protrusion.

At the end of the experiment, the length, fresh weight, and dry weight of roots, stems, and leaves were evaluated using 15 replicates. Dry weight was measured after drying the samples in a circulating air oven at 60 °C for 48 h. he soluble solids (sugar content) in mature fruits were assessed by placing a drop of juice extracted from the pulp onto a digital refractometer (ATAGO, PR- 101 model). Results were expressed in °Brix, with four replicates of six fruits per treatment.

Leaf gas exchange

At 75 days after sowing, leaf gas exchange analyses were performed on five plants per treatment using a portable infrared gas analyzer (IRGA, LICOR 6400 XT). Photosynthetically active radiation (Q) was maintained at 800 µmol m^{-2} s^{-1}, a value determined based on the incident light in the greenhouse at the time of measurement. The following parameters were assessed: net photosynthesis rate (A), stomatal conductance (gs), transpiration rate (E), and intercellular CO_2 concentration (Ci). Water use efficiency (WUE) was calculated as the ratio of A to E (A/E). All measurements were taken in the morning on the fully expanded leaf at the third node.

Chlorophyll and carotenoid contents

At 120 days, five leaf samples (5 mm^2 each) were collected per treatment. The samples were fixed in dimethyl sulfoxide (DMSO) for 12 h, protected from light

exposure. Spectrophotometric readings were then performed at wavelengths of 665 nm, 649 nm, and 480 nm [27]. The concentrations of chlorophyll a (Chl a), chlorophyll b (Chl b), and carotenoids (Car) were estimated using Eqs. (1), (2), (3), and (4).

$$\text{Chla} = 12.19 \times A_{665} - 3.45 \times A_{649} \quad (1)$$

$$\text{Chlb} = 21.99 \times A_{649} - 5.32 \times A_{665} \quad (2)$$

$$\text{Car} = 1000 \times A_{480} - 2.14 \times \text{Chla} - 70.16 \times \text{Chlb}/220 \quad (3)$$

$$\text{Chl total} = \text{Chla} + \text{Chlb} \quad (4)$$

where A is the absorbance measured at each wavelength.

Anatomical analysis

To assess potential anatomical and structural changes in the embryo and seedlings, 60 seeds per treatment underwent the same sanitization and immersion processes described earlier. The seeds were placed in plastic germination boxes lined with moistened filter paper soaked in distilled water and maintained in a growth chamber (BOD) at 25 °C.

Seed and seedling samples (six per treatment) were collected on days 1, 2, 3, 5, 6, 7, 8, 9, and 10 after germination. The samples were fixed in a modified Karnovsky solution containing 2.5% glutaraldehyde, 2.5% paraformaldehyde, and 0.05 mM $CaCl_2$ in a 0.1 M sodium cacodylate buffer (pH 7.2) for 48 h [28]. Three seeds from each treatment were subsequently dehydrated in 100% ethanol and infiltrated with hydroxyethyl methacrylate (Leica Historesin®, Heraeus Kulzer, Germany) following the manufacturer's instructions. The resulting blocks were sectioned using a rotary microtome in both longitudinal and transverse planes, with section thickness ranging from 5 to 7 µm. The obtained sections were stained with 0.05% toluidine blue in phosphate buffer and citric acid (pH 4.5) [29]. After staining, the sections were mounted on slides and covered with Entellan® synthetic resin (Merck, Germany). Images were captured using an Olympus DP71 video camera coupled to an Olympus BX51 microscope.

At 140 days, five samples from the middle region of the primary root, stem and leaf from each treatment were fixed in Karnovsky solution [28] and buffered with 4% neutral formalin for 48 h. The samples were then dehydrated in 70% ethanol and stored in glass containers. Leaf samples were further dehydrated in 100% ethanol and infiltrated with hydroxyethyl methacrylate (Leica Historesin®, Heraeus Kulzer, Germany). The resulting blocks were sectioned using a rotary microtome (Leica Biosystems, RM 2045, Germany) in both longitudinal and transverse planes, with section thickness ranging from 5 to 10 µm. The obtained sections were stained with 0.05% toluidine blue in a phosphate-citric acid buffer (pH 4.5) [29], then mounted on slides and coverslips using synthetic resin (Entellan®, Merck, Germany). The results were documented by capturing images with an Olympus DP71 video camera attached to an Olympus BX 51 microscope.

For the root and stem samples, sections from each treatment were cut using a sliding microtome (Leica Biosystems, RM 2045, Germany) with thicknesses ranging from 8 to 13 µm. These sections were also stained with 0.05% toluidine blue in a phosphate-citric acid buffer (pH 4.5) [29], and images were captured with the same Olympus DP71 video camera attached to an Olympus BX 51 microscope.

To assess the influence of auxin on secondary xylem, the number of vessels, the area of the stem vascular cylinder, the area of the leaf vascular bundles, and the area of the root vascular cylinder were measured in five replicates per treatment using ImageJ software. Additionally, the equivalent diameter of leaf, stem, and root vessel elements was calculated, with 50 replicates per treatment, following the methodology proposed by Scholz et al. [30].

LNPs in seeds: confocal microscopy analysis

The LNPs were labeled with Liss Rhod PE (1,2-dioleoyl-sn-glycero- 3-phosphoethanolamine-N- (lissamine rhodamine B sulfonyl) (ammonium salt) for absorption and localization analyses. For this purpose, the seeds were immersed in the labeled LNP solution and left under slow agitation. After 5 h, a longitudinal cut was made in the seeds, mounted on a slide with a coverslip using distilled water, and immediately analyzed via an upright confocal microscope (Zeiss, LSM780, Germany).

In the microscope, two different channels were used: one for autofluorescence absorption in white and the other for the specific wavelength range of the fluorochrome in green. The excitation wavelength employed was 552 nm, with emission detected between 572 and 607 nm for the fluorochrome, and between 430 nm and 660–680 nm for autofluorescence. The images presented in the study are composite images from both channels. These analyses were conducted at the National Institute of Photonics Applied to Cell Biology (INFABiC), at the University of Campinas (UNICAMP).

Table 1 Characterization of lignin nanoparticles (LNPs), lignin nanoparticles encapsulating IAA (LNPs-IAA) and labeled LNPs performed using dynamic light scattering (DLS). PDI refers to the polydispersity index

	Size (nm)	PDI	Zeta Potential (mV)
LNPs	201 ± 85	0.151	− 34.5
LNPs-IAA	221 ± 70	0.166	− 41.7
Labeled LNPs	228 ± 3.4	0.29	− 50

Statistical analysis

The morphometric, physiological, biochemical, and quantitative anatomical data were first subjected to the Anderson–Darling normality test. Based on the results, parametric analysis of variance (ANOVA) or nonparametric analysis (Kruskal–Wallis) was applied, depending on the data distribution. When significant differences were found, the means were compared using Tukey's or Dunn's post hoc tests, with a significance level set at 5%. All analyses were conducted using R software. The mean values for each measured parameter are provided in supplementary Table 2.

Results

Table 1 presents the characterization of lignin nanoparticles (LNPs), labeled lignin nanoparticles, and lignin nanoparticles encapsulating IAA (LNPs-IAA). The encapsulation efficiency was 90%. The results indicate that the nanoparticles had an average size of approximately 200 nm and exhibited low polydispersity. The addition of IAA or fluorochrome did not affect the colloidal properties of the nanoparticles. The release profile evaluation demonstrated that lignin nanoparticles facilitate a sustained release of IAA (Fig.Sup. 2). After 8 h, approximately 40% of the IAA was released, with the release reaching around 55% after 24 h.

The labeled LNPs were detected after 5 h of immersion, primarily in the seed coat, endosperm, embryo, and cotyledons (Fig. 1). Control sections were prepared in the same regions and observed under the same wavelength (Fig. 1a, c, f, h, j). The LNPs exhibited aggregation behavior and were found on the surface of the hairy seed coat (Fig. 1b). In the endosperm, LNPs were observed in the apoplastic region (Fig. 1d) and within the cells (Fig. 1e). In the embryo, particularly in the radicle sector, some LNPs were found inside the cells (Fig. 1g). In the cotyledon region (Fig. 1i), fewer nanoparticles were observed. However, they were present between the cotyledons (Fig. 1i), inside the cotyledons, and within the endosperm

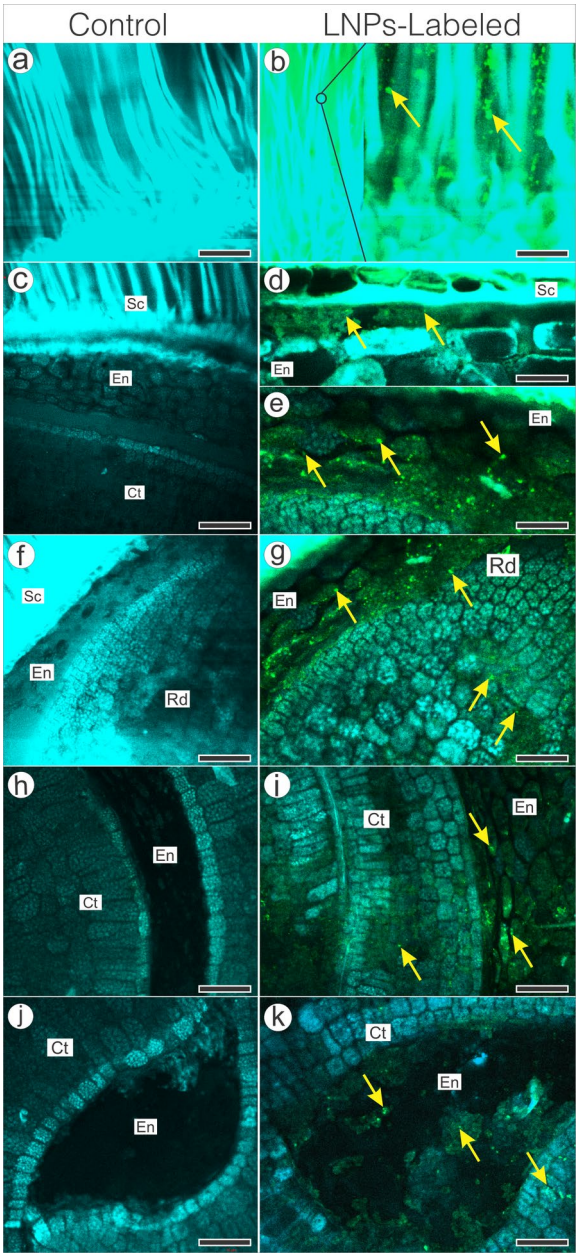

Fig. 1 Confocal images of the seed coat, endosperm, embryo, and cotyledons of cherry tomato plants after 5 h of immersion in a solution containing lignin nanoparticles labeled with lissamine rhodamine B sulfonyl chloride (ex: 552 nm; em: 572—607 nm). The seed coat with non-glandular trichomes is shown in both the control (**a**) and LNP-labeled (**b**) samples. The endosperm of control seeds (**c**) and those labeled with LNPs (**d**, **e**) show the nanoparticles inside and between cells. The radicle region in control sections (**f**) and LNP-labeled sections (**g**) is depicted. Cotyledons and the endosperm region in control sections (**h**, **j**) and LNP-labeled sections (**i**, **k**). The yellow arrows indicate the presence of LNPs. The analysis was performed on five seeds. Ct = cotyledon; En = endosperm; Hp = hypocotyl; Rd = radicle; Sc = seed coat. Bars: 20 µm

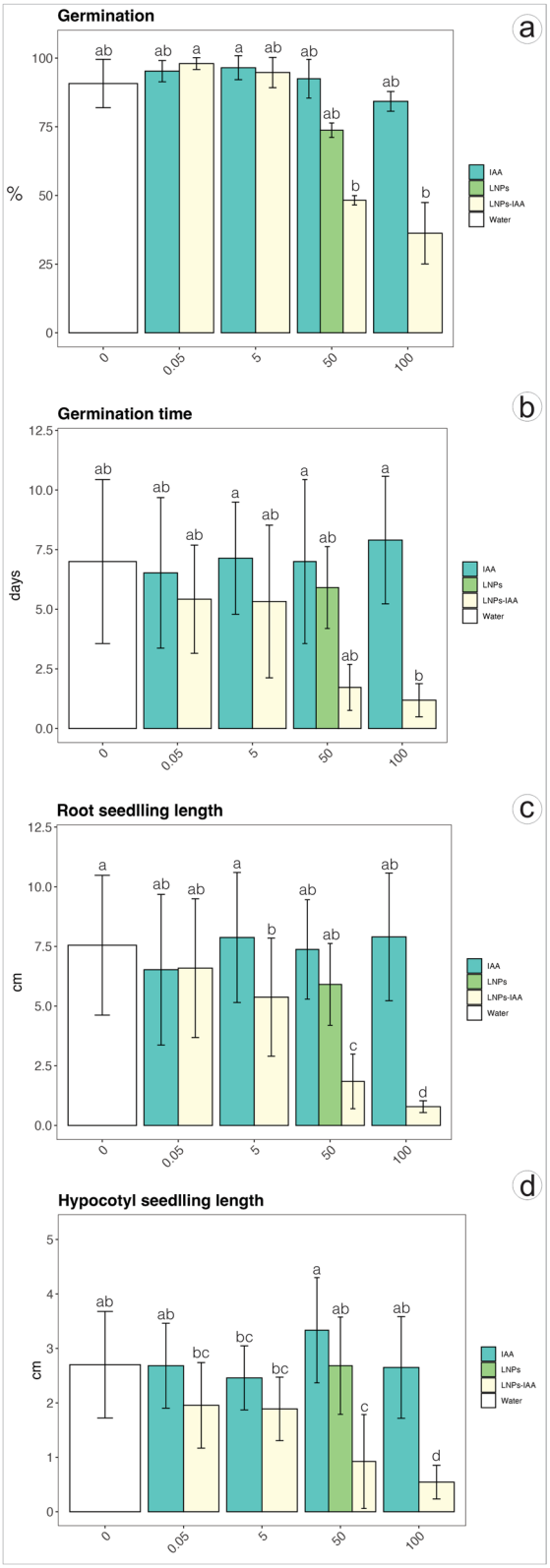

◀ **Fig. 2** Germination and seedling parameters of cherry tomato plants after 10 days of cultivation before adding auxin encapsulated in lignin nanoparticles (LNPs-IAA) and its free form (IAA) at concentrations of 0.05, 5, 50, and 100 µg/mL. (**a**, **b**) Germination time and rate. (**c**, **d**) Seedling parameter measurements. (**e**) Seedling morphology in all the treatment groups. All the data were subjected to parametric analysis of variance (ANOVA) and compared via the Tukey test at the 5% significance level in RStudio software. Bars: 1 cm

cells in the middle region of the seeds (Fig. 1k). The control section containing only LNPs-labeled samples is provided in Supplementary Fig. 02.

The germination rates were not significantly affected by treatments with LNPs and LNPs-IAA, as shown in Fig. 2a. However, a trend was observed, with germination rates being lower and the time required for germination being prolonged at higher concentrations of LNPs-IAA (Fig. 2b). This extended germination time was also noted in the LNPs treatment without IAA.

The LNPs-IAA at concentrations of 50 and 100 µg mL^{-1} resulted in significant reductions in both root and hypocotyl lengths compared to the control treatment (Fig. 2c, d). Regarding seedling morphology (Fig.Sup. 03), no alterations or phytotoxic effects were observed in most treatments, except for the LNPs-IAA 100 µg mL^{-1} treatment, where the seedlings difficult to fully develop even after ten days of germination.

The anatomical analysis of seedling development during the first 10 days of the experiment revealed no significant differences in seed/seedling structure among the treatments, except for the timing of root protrusion and hypocotyl formation (Fig. 3). The germination process in all treatments, except for LNPs and LNPs-IAA 50 and 100 µg mL^{-1}, began with the seed coat protruding to allow root emergence on the 2nd day (Fig. 3b). By the 3rd day (Fig. 3c), root elongation started, and cotyledon opening occurred between the 4 th and 5 th days (Fig. 3d). By the 10 th day, root elongation continued, and the apical meristem (MAC) was fully differentiated (Fig. 3e). In the treatments with LNPs and LNPs-IAA 50 µg mL^{-1}, root protrusion began only on the 3rd day (Fig. 3h), followed by root elongation (Fig. 3i, j). The LNPs-IAA 100 µg mL^{-1} caused root protrusion only on the 5 th or 6 th day (Fig. 3p). By the 10 th day, root elongation was still ongoing, and cotyledon opening had not yet occurred (Fig. 3q). In the rest of treatments, cotyledon opening and MAC formation were similar (Fig. 3k).

After 140 days of cultivation, the number of leaves tended to increase with higher concentrations; however, no significant differences were observed compared to the control, except for LNPs-IAA 0.05 µg mL^{-1}, which resulted in a reduction in this variable (Fig. 4a). On the other hand, LNP-IAA 100 µg mL^{-1} and IAA 100 µg

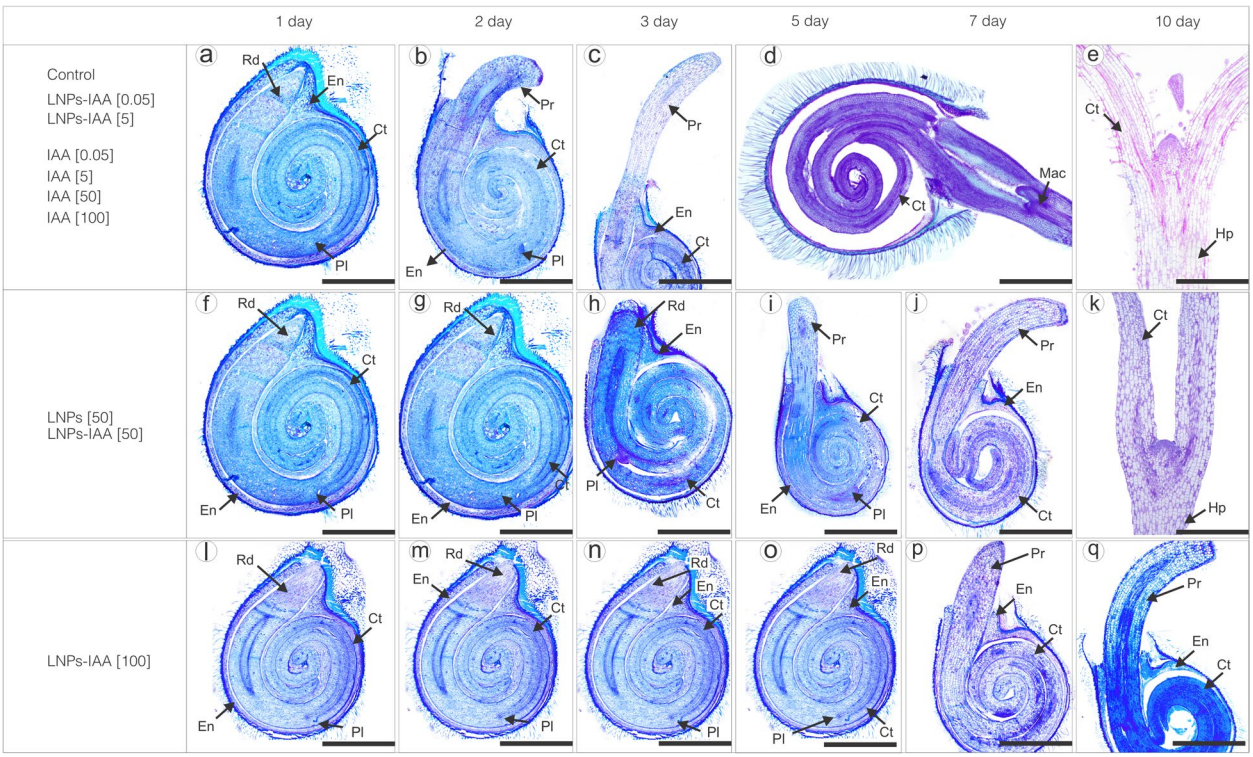

Fig. 3 Light photomicrographs of seed germination and seedling formation at 10 days of development. No alterations in embryo structure were observed in the seeds (a, f, l, g, h, m, n, o). Root protrusion from the seed coat marked the beginning of the germination process (b, i, p). Root elongation followed (c, j, q), along with the initial stages of cotyledon opening (d). Fully developed seedlings were observed 10 days after germination (e, k). Ct = cotyledon; En = endosperm; Hp = hypocotyl; MAC = shoot apical meristem; Pr = primary root; Rd = radicle. Scale bars: 500 µm

mL^{-1} induced the shortest stem length (Fig. 4b). For root length (Fig. 4c), no significant differences were observed among treatments. However, fresh leaf weight increased when seeds were treated with LNP-IAA 100 µg mL^{-1} and IAA 100 µg mL^{-1} (Fig. 4d). Additionally, root fresh and dry weight were higher under LNP-IAA 100 µg mL^{-1} and IAA 100 µg mL^{-1} treatments (Fig. 4e, f). These differences were primarily associated with the presence of adventitious and lateral roots compared to the other treatments (Fig. 4j).

In the physiological parameters, IAA 0.05 µg mL^{-1} and 5 µg mL^{-1} showed the highest photosynthesis rates (Fig. 4g), while LNPs-IAA 100 µg mL^{-1} exhibited the lowest rates. However, no treatment showed a significant difference. A similar trend was observed for water use efficiency (Fig.Sup. 4f) and transpiration (Fig. Sup. 4d). LNPs-IAA 100 µg mL^{-1} resulted in the lowest stomatal conductance (Fig. 4h) and the lowest intercellular CO_2 concentration (Fig.Sup. 4e). Leaf concentrations of total chlorophyll and carotenoids were reduced when applying LNPs-IAA 100 µg mL^{-1} and IAA 100 µg mL^{-1} (Fig. 4i; Fig.Sup. 4i).

The application of LNPs and LNPs-IAA did not affect the internal morphology of leaves, stems, or roots (Fig. Sup. 5a–p). However, the quantitative analysis of xylem tissue traits revealed significant effects (Fig. 5). LNPs-IAA and IAA at 0.05 and 5 µg mL^{-1} reduced the total xylem area in leaves (Fig. 5a), whereas, LNPs-IAA, and IAA at 100 µg mL^{-1} increased the xylem area in stems (Fig. 5e). In the roots (Fig. 5i), LNPs-IAA at 0.05 µg mL^{-1} and IAA at 5 µg mL^{-1} increased the total xylem area, whereas IAA and LNPs-IAA at 100 µg mL^{-1} drastically reduced it.

The number of vessels in leaves (Fig. 5b) was influenced by most treatments, except for LNPs at 50 µg mL^{-1} and LNPs-IAA at 0.05 µg mL^{-1}. In the stem (Fig. 5f), no significant differences were observed among the treatments. For the roots (Fig. 5j), IAA at 5 µg mL^{-1} showed the highest number of vessels, whereas both treatments with 100 µg mL^{-1} resulted in a drastic reduction.

Regarding the equivalent diameter of vessels, LNPs-IAA at 0.05 µg mL^{-1} increased vessel diameter in leaves (Fig. 5c), while LNPs-IAA at 5 µg mL^{-1} reduced it. In stems, LNPs-IAA at 0.05 and 5 µg mL^{-1} increased vessel

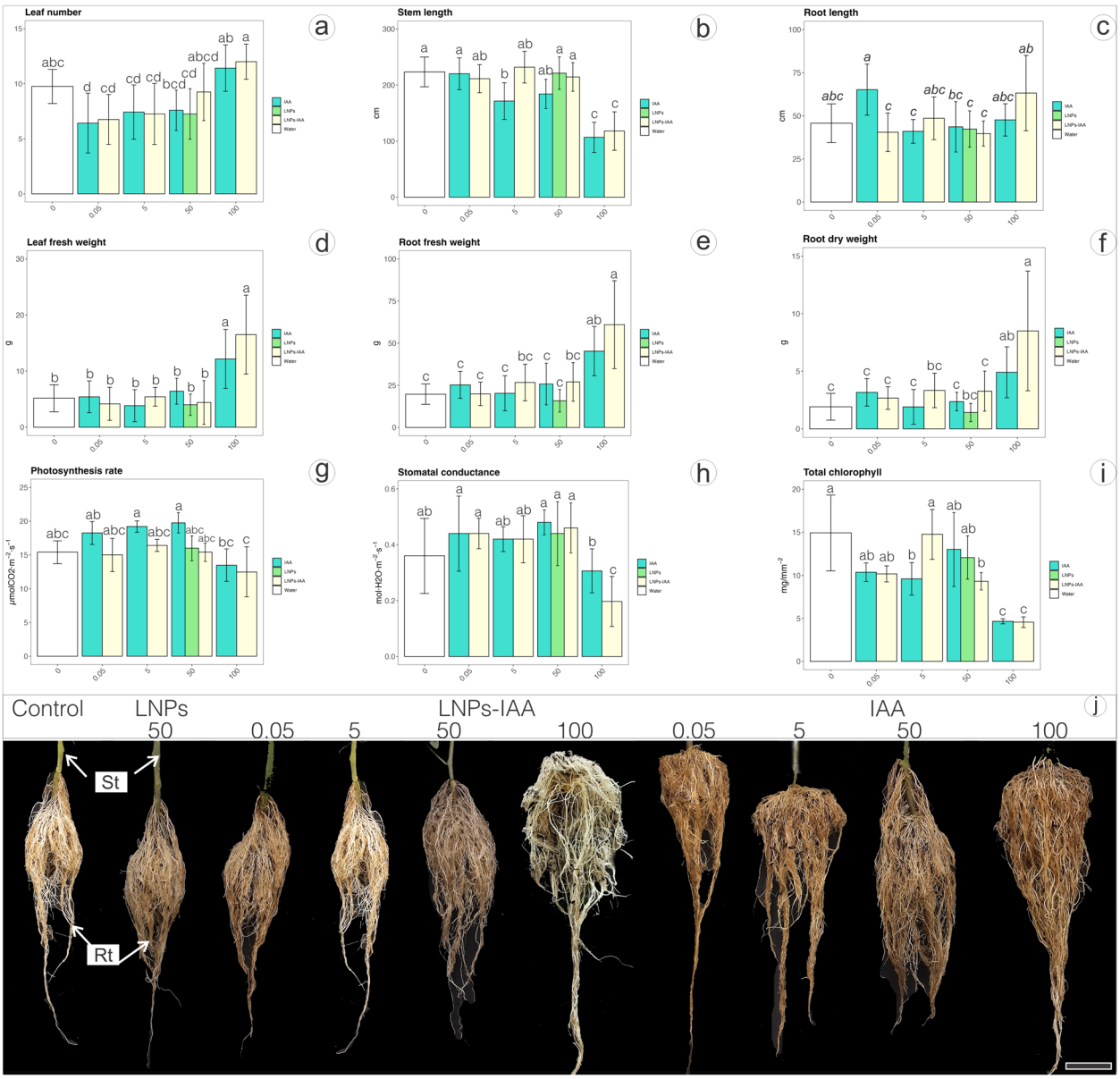

Fig. 4 Morphometric (**a**, **b**, **c**, **d**, **e**, **f**), physiological (**g**, **h**), biochemical (**i**), and morphological (**j**) parameters of adult cherry tomato plants cultivated for 140 days after the application of auxin encapsulated in lignin nanoparticles (LNPs-IAA) and its free form (IAA) at concentrations of 0.05, 5, 50, and 100 µg/mL. All data were subjected to nonparametric Kruskal–Walli's analysis of variance and compared via the Duncan test at a 5% significance level using RStudio software. Bars: 5 cm

diameter (Fig. 5g), whereas LNPs-IAA at 100 µg mL^{-1} led to a reduction. The vessel diameter in roots was not affected by any treatments (Fig. 5k).

After 140 days, Table 2 presents the total number of fruits produced under each treatment. Compared to the control and LNPs, LNPs-IAA at 0.05 µg mL^{-1} resulted in the highest fruit count. In contrast, fruit sugar content was reduced in treatments with LNPs-IAA at 100 µg mL^{-1} and IAA at 50 µg mL^{-1} compared to the control.

Discussion

The results demonstrate that lignin nanoparticles (LNPs) were effectively absorbed by plants without inducing morphological alterations in vegetative or reproductive structures throughout the life cycle. The encapsulation efficiency of auxin in LNPs was comparable to free-hormone treatments, confirming the effectiveness of lignin nanoparticles as delivery systems. Furthermore, the chemical composition of the nanoparticles influenced

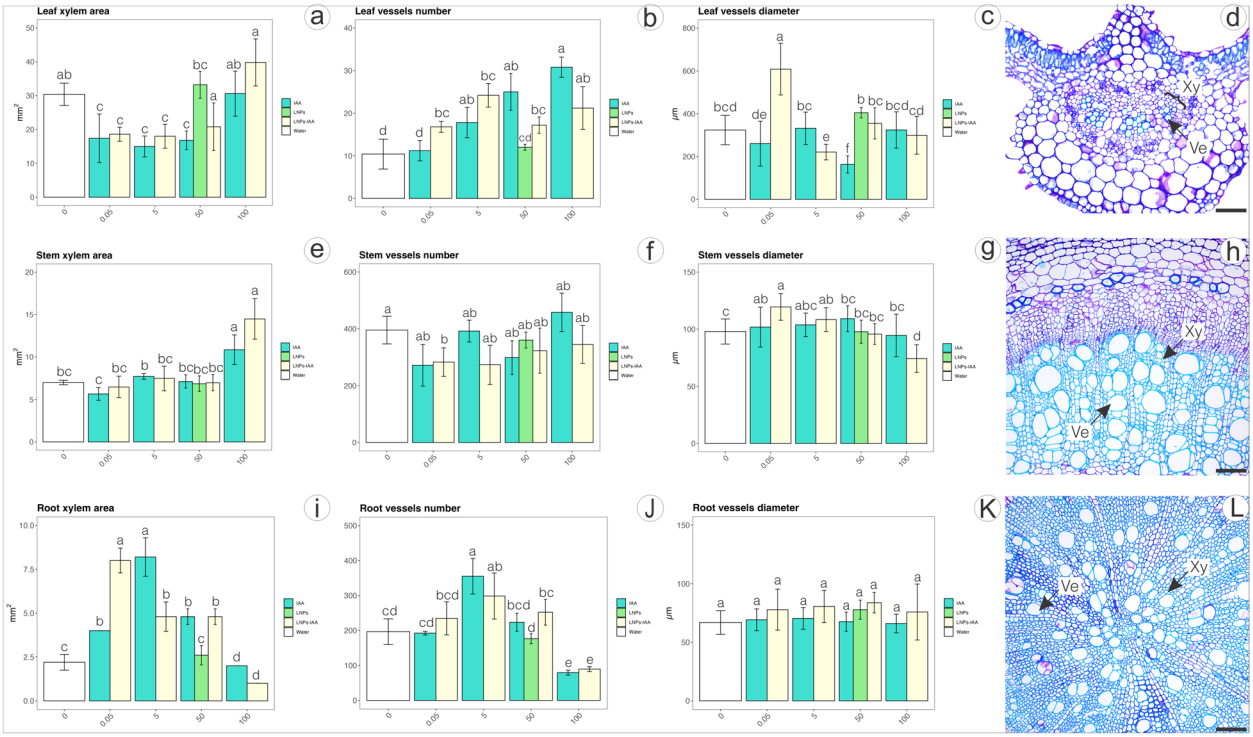

Fig. 5 Xylem quantitative parameters in cherry tomatoes at 130 days of cultivation after applying auxins encapsulated in lignin nanoparticles and their free form at concentrations of 0.05, 5, 50, and 100 µg/mL. Leaf parameters (**a**, **b**, **c**, **d**), stem parameters (**e**, **f**, **g**, **h**) and root parameters (**i**, **j**, **k**, **L**). All the data were subjected to nonparametric Kruskal–Walli's analysis of variance and compared via the Duncan test at the 5% significance level in RStudio software. Xy = xylem. Ve = vessels. Bars: 100 µm

Table 2 Number of total fruits and sugar contents (ºBrix) produced by the tomato plants after 140 days of cultivation. All the data were subjected to analysis of variance (ANOVA) and compared via the Tukey test at the 5% significance level in RStudio software

Treatments	Total fruit number	Soluble solids (%)
Control	320 ± 13 bc	8.2 ± 1 a
LNPs	339 ± 14 b	7.4 ± 0.5 ab
LNPs-IAA 0.05	460 ± 10 a	7.9 ± 1.4 a
LNPS-IAA 5	410 ± 15 ab	7.6 ± 1.6 ab
LNPS-IAA 50	372 ± 15 b	7.4 ± 1 ab
LNPs-IAA 100	279 ± 12 c	6.8 ± 0.8 b
IAA 0.05	350 ± 10 b	6.8 ± 1.9 ab
IAA 5	295 ± 13 bc	7,1 ± 0.2 ab
IAA 50	442 ± 15 ab	6.7 ± 0.6 b
IAA 100	285 ± 10 c	7.2 ± 1 ab

seed germination parameters. At lower concentrations, LNPs-IAA treatments showed minimal statistical differences in growth promotion parameters compared to free IAA, particularly in xylem development and fruit yield. However, higher concentrations elicited phytotoxic effects, including significant reduction in chlorophyll content, impaired gas exchange and decreased fruit number.

While Falsini et al. [13] previously reported LNP localization in tomato seed coats after 48 h and root absorption after 72 h, our findings demonstrate significantly faster uptake kinetics. We observed LNP internalization and cellular absorption within just 5 h of exposure, confirming the rapid transport capacity of these nanoparticles throughout plant tissues. This accelerated uptake profile highlights the potential of LNPs for efficient delivery of bioactive compounds in agricultural applications.

The occurrence of trichomes efficiently assists in the adhesion of LNPs to the seed coat. Although the presence of LNPs in association with trichomes has been reported, the role of these structures in nanoparticle internalization has not been confirmed [31]. Trichomes are structures that have already been reported as excellent immobilizers of nanoparticles, but it is still unclear whether these structures are part of any absorption pathway [31]. The transport of LNPs observed in seeds is primarily apoplastic, which is considered one of the main

routes of nanoparticle translocation in higher plants [32]. This type of transport aligns with the characteristics of LNPs, which are 200–220 nm in length, making symplastic transport difficult, as plasmodesmata do not have pores larger than 2–20 nm [31]. Additionally, the negative charge of LNPs could facilitate apoplastic and xylem transport, as cell walls generally carry the same charge [33].

The cellular internalization of LNPs remains a challenge. Although we report the presence of LNPs within endosperm cells, radicles, and cotyledons, the method of their absorption into the cell protoplast is still unknown. However, Avellan and collaborators [31] highlighted that this process may occur through passive diffusion, such as membrane traversal, or transient pores, like water channels and aquaporins [34]. Similarly, active diffusion may occur through endocytosis processes or protein carriers. Endocytosis is a highly viable pathway for the absorption of extracellular molecules [31], as protoplasts can internalize particles up to 1 µm in size, mainly for delivering specific material into organelles. In contrast, delivery into the cytosol and pore opening in the membrane seems to be the most appropriate pathways [35]. Furthermore, nanoparticles can be taken up through both hydrophobic and hydrophilic interactions. Lignin, being a biopolymer, exhibits both characteristics, which may enable the uptake of lignin nanoparticles from the seed teguments, which are lignified and possess hydrophobic properties.

Our findings revealed no significant impact of the treatments on germination rates, contrasting with previous studies demonstrating enhanced germination at low concentrations of polymeric nanoparticles [17, 18, 20]. Notably, we observed no synergistic effect between auxins and nanoparticles on germination, despite established literature documenting auxin-mediated stimulation of cell division and elongation during early seedling development [23]. Notably, we observed concentration-dependent germination inhibition, with higher concentrations of both LNPs and LNPs-IAA significantly reducing germination rates and increasing germination time. These findings align with studies using poly(ε-caprolactone) (PCL) nanocapsules, where nanoparticle uptake was shown to modify seed water potential, ultimately delaying germination and impairing seedling establishment in Brassica species [36]. Studies with maize seeds have shown that high concentrations of lignin nanoparticles (LNPs) delayed germination and caused phytotoxic effects [12]. The authors suggest these effects are likely related to lignin constituents (p-hydroxyphenyl, guaiacyl, and syringyl), which have been previously documented as plant growth inhibitors [37].

An alternative explanation for the observed germination inhibition and delayed germination rates may involve the presence of carvacrol in the LNP composition. This essential oil component, present in our treatments at approximately 4 µg/mL, has been previously documented as a potent pesticide across multiple plant species [38, 39]. Studies report that carvacrol application—whether through foliar sprays or seed treatment—can completely inhibit germination and impair seedling development. Notably, concentrations as low as 3 µg/mL have demonstrated herbicidal activity in sensitive species.

After 140 days of cultivation, our analysis revealed that hormone encapsulation in LNPs at low dosages did not significantly affect growth. However, at higher dosages, there was a notable influence on stem and root parameters. Specifically, stem length decreased, whereas root parameters, such as fresh and dry weights, significantly increased. These stem and root results can be explained by ethylene biosynthesis being mediated by high IAA concentrations. Elevated levels of IAA can stimulate ethylene biosynthesis, which may inhibit specific developmental processes, particularly in the hypocotyl region [40–42]. Maintaining low levels of ethylene during the vegetative phases of plant growth is crucial, as high concentrations can adversely affect stem elongation [41]. Indeed, ethylene has a significant effect on increasing root biomass [43, 44], particularly in lateral roots. This aligns with our findings where LNPs-IAA and IAA 100 µg mL^{-1} treatments were observed to influence lateral root development, leading to an increase in root mass.

Regarding leaf gas exchange, no significant differences were observed in the physiological parameters for the LNP-IAA treatments at low dosages. However, at high dosages, a significant reduction was noted. The decrease in photosynthesis and CO_2 concentration can be attributed to lower stomatal conductance values (gs), particularly in the LNP-IAA 100 µg mL^{-1} treatment. In the same concentration, a reduction in leaf contents of chlorophyll and carotenoids was also observed. These results suggest that the plants may be experiencing oxidative stress related to the high levels of IAA exposure, with the IAA 100 µg mL^{-1} treatment showing similar effects. Oxidative stress can impair photosynthetic efficiency and disrupt pigment synthesis, leading to reduced photosynthesis and overall plant productivity [45].

Previous studies with different plant species have also indicated that high concentrations of IAA can trigger various stress responses during plant development, including oxidative stress [40, 46, 47]. Because auxins interact with a wide range of other PGRs, primarily abscisic acid (ABA) and ethylene, it is difficult to determine phytotoxic effects precisely [23]. Reports indicate

that high levels of IAA result in responses leading to ABA accumulation in shoot tissues [48, 40]. This accumulation subsequently leads to reduced stem elongation, stomatal closure, and the accumulation of reactive oxygen species (ROS), which can contribute to oxidative stress [49, 50].

Anatomical analyses of vegetative organs demonstrated that LNP application did not alter plant structure. Our study represents the first report of such analyses. Most documented toxic effects in literature are linked to metallic nanoparticles, which have been shown to cause cell wall loosening in stems and roots, trichome shedding from leaf surfaces and growth interruption [5, 51–53]. Our results indicate that lignin-based nanoparticles did not display comparable toxicity levels, suggesting that polymeric nanoparticles may interact differently with plant tissues.

However, in the treatments where IAA free or encapsulated were used, an influence on xylem tissue development was observed, with distinct responses depending on the concentration employed. The xylem is the tissue responsible for transporting water and minerals from the roots to the photosynthetic sites in leaf tissues, as well as providing excellent mechanical resistance to plants, allowing the colonization of various environments [54]. The initiation of the xylem from procambial or cambial meristematic cells is mediated by auxins [55, 56]. The role of the auxin gradient in hormonal flux formation through PIN transporters in meristems has been widely reported in the literature, especially in vascular cambium cell division and proliferation [57].

The low-dose LNP-IAA treatments showed strong correlation with root xylem development, specifically regarding xylem area and vessel number. Multiple studies have documented the influence of both exogenous and endogenous auxins on xylem cell differentiation and development, supporting our observations [58–62]. However, high concentrations demonstrated antagonistic effects. These results correspond with our morphological analysis, where both 100 μg mL^{-1} treatments induced: increased lateral root formation and consequently reduced primary root thickness. This architectural modification may have contributed to the observed xylem area reduction. Such adaptation likely represents a stress response to high auxin concentration, potentially associated with enhanced ethylene biosynthesis and ABA accumulation. Existing literature reports that nanoparticle seed treatments can modify gene expression patterns, thereby regulating multiple metabolic responses—including phytohormone signaling pathways and concentration gradients [14, 19].

In terms of the number of fruits produced, the low-dose LNP-IAA treatment had a significantly more significant effect than the other treatments. These results are consistent with previous data from Pereira et. al. [17], where the encapsulation of GA_3 increased tomato fruit production by up to 225% with CS/TPP nanoparticles and 148% with CS/ALG nanoparticles. The authors suggest that the sustainable delivery of PGRs encapsulated, over a prolonged period compared to free release, increased fruit production, influenced by the beneficious on growth parameters such as root and stem biomass.

Based on our results, we cannot draw the same conclusions. Although the treatment with 0.05 μg mL^{-1} LNPs-IAA yielded a higher number of fruits, these findings were not supported by other morphological, physiological, or biochemical variables. The plants subjected to this treatment exhibited a significant increase in root xylem, which could potentially affect water absorption. However, the photosynthetic rates and CO2 concentration did not show any notable responses. In contrast, the 100 μg mL^{-1} LNPs-IAA reduced stomatal conductance and photosynthetic pigment levels, which may have contributed to the lower final fruit number.

Beyond that, our experiments did not evaluate fruit productivity, which are crucial factors in determining treatment efficacy. Finally, we did not measure the endogenous levels of PGRs, and such analysis demonstrating would be important to validate some of the plant growth responses we observed.

These results underscore the need for further investigation, particularly regarding the following considerations:

1) For a comprehensive understanding of polymeric nanoparticle effects, future studies should assess the complete life cycle of the target species—from germination to fruit production. Current research on polymeric nanoparticles predominantly focuses only on early developmental stages (germination and seedling growth), leaving a critical knowledge gap regarding later phases such as flowering and yield.
2) For studies employing encapsulated growth regulators, we strongly recommend concurrent biochemical profiling of endogenous phytohormone levels. This approach is critical because, as demonstrated in our study, the observed phenotypic responses frequently resulted from complex interactions between multiple PGRs rather than isolated effects.
3) Xylem development should be analyzed from its early stages to determine whether auxin-mediated growth promotion mechanisms are maintained when auxins are encapsulated in nanoparticles.
4) Future studies should incorporate comprehensive analyses of fruit/grain chemistry and physical prop-

erties, along with precise biomass measurements and productivity assessments. This multidimensional approach is essential to accurately determine the effects of different nanoparticle concentrations and formulations.

Conclusion

The evaluated lignin nanoparticles showed promising potential as nanocarriers for plant growth regulators (PGRs), producing equivalent results to the isolated application of the hormone. Additionally, our findings demonstrated that nanoparticles with lengths of 200–220 nm were readily absorbed by seeds after just five hours of immersion. Although we observed that the lowest concentration of the encapsulated hormone increased the number of fruits, the other variables did not support these results. Conversely, at higher concentrations, toxic effects contributed to a reduction in fruit number. Therefore, future studies should investigate lower concentrations of the encapsulated hormone to provide precise usage recommendations, justifying the encapsulation of bioactive compounds. Our research highlights and reinforces the importance of proper dosage and the chemical composition of nanocarriers for agricultural applications.

Supplementary Information

The online version contains supplementary material available at https://doi.org/10.1186/s12870-025-06539-1.

Supplementary Material 1.

Acknowledgements
Rodrigo Faleiro thanks the São Paulo State Research Support Foundation (FAPESP) for a doctorate scholarship (2022/02559 - 4). Leonardo F. Fraceto thanks the São Paulo State Research Support Foundation (FAPESP, grants CBioClima—#2021/10639 - 5 and #2017/21004 - 5), the Brazilian National Council for Scientific and Technological Development (CNPq-MCTI-INCT NanoAgro #405924/2022 - 4, #308439/2021 - 0) and the Coordenação de Aperfeiçoamento de Pessoal de Nível Superior – Brazil (CAPES-MEC INCTNanoAgro #88887.953443/2024 - 00). Juliana Mayer thanks CNPq (productivity grant 309175/2023 - 2). We also thank Dr. Aline Bombo, Dr. Halley Oliveira and Dr. Alejandro Perez for the review and dates discussed.

Authors' contributions
R. F: Conceptualization; anatomical, physiological, biochemical, morphometric and confocal analyses; writing—original draft; writing—review & editing. M. T: Conceptualization, fruit trait analyses, writing—review & editing. A. P: Nanoparticle production and characterization, Writing—review & editing. L. F: Nanoparticle production and characterization, Writing—review & editing. M. R: Morphometric and Physiological analyses. F.C: Biochemical analyses. M.M: Physiological analyses. M.P: Physiological analyses. R.R: Physiological analyses, Writing—review & editing. J.M: Conceptualization, Writing—original draft, Writing—review & editing.

Funding
These works are funded by the São Paulo Research Foundation (FAPESP), the National Council for Scientific and Technological Development (CNPq) and Coordenação de Aperfeiçoamento de Pessoal de Nível Superior (Capes) – Brazil.

Data availability
All data mean values used for the variables presented in this article for each treatment are available in the supplementary material on table format.

Declarations

Ethics approval and consent to participate
Not applicable.

Consent for publication
Not applicable.

Competing interests
The authors declare no competing interests.

Author details
[1]Departamento de Botánica, Instituto de Biología, Universidad Nacional Autómoma de México, Circuito Zona Deportiva, Ciudad UniversitariaCoyoacán, Mexico City, México. [2]Laboratorio de Pós-Colheita, Departamento de Ciências Biológicas, Escola Superior de Agricultura "Luiz de Queiroz", Piracicaba, Brasil. [3]Institute of Science and Technology of Sorocaba, Department of Environmental Engineering, São Paulo State University – Unesp,, Sorocaba, Brazil. [4]B. nano Soluções Tecnológicas. Av. Itavuvu, 11.777 - Jardim Santa Cecilia, 18078 - 005 Sorocaba, SP, Brasil. [5]Department of Plant Physiology, Umeå University, Umea, Sweden. [6]Laboratory of Crop Physiology (LCroP), Department of Plant Biology, Institute of Biology, Universidade Estadual de Campinas, Campinas, SP, Brazil. [7]Departamento de Ciências Biológicas, Universidade Federal de Santa Catarina, Florianópolis, Brasil. [8]Laboratório de Anatomia Vegetal, Departamento de Biologia Vegetal, Instituto de Biologia, Universidade Estadual de Campinas, Campinas, Brasil.

Received: 10 February 2025 Accepted: 10 April 2025
Published online: 05 June 2025

References

1. Athanassiou CG, Kavallieratos NG, Benelli G, Losic D, Usha Rani P, Desneux N. Nanoparticles for pest control: current status and future perspectives. J Pest Sci. 2004;2018(91):1–15.
2. Bombo AB, Pereira AES, Lusa MG, de Medeiros OE, de Oliveira JL, Campos EVR, et al. A Mechanistic view of interactions of a nanoherbicide with target organism. J Agric Food Chem. 2019;67:4453–62.
3. Fraceto LF, Grillo R, de Medeiros GA, Scognamiglio V, Rea G, Bartolucci C. Nanotechnology in agriculture: Which innovation potential does it have? Front Environ Sci. 2016;4. https://doi.org/10.3389/fenvs.2016.00020.
4. da Silva VHC, de Lima RF, Mayer JLS, Arruda MAZ. Feasibility of using silica (Na2SiO3 and SiO2NPs) to mitigate mercury in transgenic soybeans grown in contaminated soils and respective effects on nutrient homeostasis. Environ Sci Pollut Res. 2025;32:7600–19.
5. Quintela AL, Santos MFC, de Lima RF, Mayer JLS, Marcheafave GG, Arruda MAZ, et al. Influence of Silver Nanoparticles on the Metabolites of Two Transgenic Soybean Varieties: An NMR-Based Metabolomics Approach. J Agric Food Chem. 2024;72:12281–94.
6. Zhang Y, Ni S, Wang X, Zhang W, Lagerquist L, Qin M, et al. Ultrafast adsorption of heavy metal ions onto functionalized lignin-based hybrid magnetic nanoparticles. Chem Eng J. 2019;372:82–91.
7. Thomas S, Shanks R, Joy J. Micro and Nanostructured Polymer Systems: From Synthesis to Applications. 1st ed. Inc.: CRC Press; 2016.
8. Auffan M, Rose J, Bottero J-Y, Lowry GV, Jolivet J-P, Wiesner MR. Towards a definition of inorganic nanoparticles from an environmental, health and safety perspective. Nat Nanotechnol. 2009;4:634–41.
9. Campos EVR, do Espirito Santo Pereira A, de Oliveira JL, Villarreal GPU, Fraceto LF. Nature-Based Nanocarrier System: An Eco-friendly Alternative for Improving Crop Resilience to Climate Changes. Anthropocene Science. 2022;1:396–403.
10. Low LE, Teh KC, Siva SP, Chew IML, Mwangi WW, Chew CL, et al. Lignin nanoparticles: The next green nanoreinforcer with wide opportunity. Environ Nanotechnol Monit Manag. 2021;15:100398.

11. Pereira A do ES, Luiz de Oliveira J, Maira Savassa S, Barbara Rogério C, Araujo de Medeiros G, Fraceto LF. Lignin nanoparticles: New insights for a sustainable agriculture. J Clean Prod. 2022;345:131145.
12. Del Buono D, Luzi F, Puglia D. Lignin Nanoparticles: A promising tool to improve Maize physiological, biochemical, and Chemical Traits. Nanomaterials. 2021;11:846.
13. Falsini S, Clemente I, Papini A, Tani C, Schiff S, Salvatici MC, et al. When Sustainable Nanochemistry Meets Agriculture: Lignin Nanocapsules for Bioactive Compound Delivery to Plantlets. ACS Sustain Chem Eng. 2019;7:19935–42.
14. do Espirito Santo Pereira A, Caixeta Oliveira H, Fernandes Fraceto L, Santaella C. Nanotechnology Potential in Seed Priming for Sustainable Agriculture. Nanomaterials. 2021;11:267. https://doi.org/10.3390/nano11020267.
15. Tiwari K, Tripathi S, Mahra S, Mathew S, Rana S, Tripathi DK, et al. Carrier-based delivery system of phytohormones in plants: stepping outside of the ordinary. Physiol Plant. 2024;176. https://doi.org/10.3390/nano11020267.
16. Sampedro-Guerrero J, Vives-Peris V, Gomez-Cadenas A, Clausell-Terol C. Encapsulation Reduces the Deleterious Effects of Salicylic Acid Treatments on Root Growth and Gravitropic Response. Int J Mol Sci. 2022;23:14019.
17. Pereira A do ES, Oliveira HC, Fraceto LF. Polymeric nanoparticles as an alternative for application of gibberellic acid in sustainable agriculture: a field study. Sci Rep. 2019;9:7135.
18. Pereira AES, Silva PM, Oliveira JL, Oliveira HC, Fraceto LF. Chitosan nanoparticles as carrier systems for the plant growth hormone gibberellic acid. Colloids Surf B Biointerfaces. 2017;150:141–52.
19. Fregonezi BF, Pereira AES, Ferreira JM, Fraceto LF, Gomes DG, Oliveira HC. Seed Priming with Nanoencapsulated Gibberellic Acid Triggers Beneficial Morphophysiological and Biochemical Responses of Tomato Plants under Different Water Conditions. Agronomy. 2024;14:588.
20. Pereira AES, Sandoval-Herrera IE, Zavala-Betancourt SA, Oliveira HC, Ledezma-Pérez AS, Romero J, et al. γ-Polyglutamic acid/chitosan nanoparticles for the plant growth regulator gibberellic acid: Characterization and evaluation of biological activity. Carbohydr Polym. 2017;157:1862–73.
21. Rademacher W. Plant Growth Regulators: Backgrounds and uses in plant production. J Plant Growth Regul. 2015;34:845–72.
22. Small CC, Degenhardt D. Plant growth regulators for enhancing revegetation success in reclamation: A review. Ecol Eng. 2018;118:43–51.
23. Paque S, Weijers D. Auxin: the plant molecule that influences almost anything. BMC Biol. 2016;14:67.
24. Miransari M, Smith DL. Plant hormones and seed germination. Environ Exp Bot. 2014;99:110–21.
25. Grossmann K. Auxin herbicides: current status of mechanism and mode of action. Pest Manag Sci. 2010;66:113–20.
26. Srinivasan TS. Phytohormones and crosstalk among biotic stress responsive signaling pathways in plants. Proc Indian Natl Sci Acad. 2024. https://doi.org/10.1007/s43538-024-00294-x.
27. Wellburn AR. The Spectral determination of chlorophylls a and b, as well as total carotenoids, using various solvents with spectrophotometers of different resolution. J Plant Physiol. 1994;144:307–13.
28. Karnovsky MJ. A Formaldehyde-Glutaraldehyde Fixative of High Osmolality for Use in Electron Microscopy. J Cell Biol. 1965;27:137–8.
29. Sakai WS. Simple method for differential staining of paraffin embedded plant material using Toluidine Blue O. Stain Technol. 1973;48:247–9.
30. Scholz A, Klepsch M, Karimi Z, Jansen S. How to quantify conduits in wood? Front Plant Sci. 2013;4:56. https://doi.org/10.3389/fpls.2013.00056.
31. Avellan A, Yun J, Morais BP, Clement ET, Rodrigues SM, Lowry GV. Critical Review: Role of Inorganic Nanoparticle Properties on Their Foliar Uptake and *in Planta* Translocation. Environ Sci Technol. 2021;55:13417–31.
32. Azim Z, Singh NB, Singh A, Amist N, Niharika, Khare S, et al. A review summarizing uptake, translocation and accumulation of nanoparticles within the plants: current status and future prospectus. J Plant Biochem Biotechnol. 2023;32:211–24.
33. Zhang Y, Martinez MR, Sun H, Sun M, Yin R, Yan J, et al. Charge, Aspect Ratio, and Plant Species Affect Uptake Efficiency and Translocation of Polymeric Agrochemical Nanocarriers. Environ Sci Technol. 2023;57:8269–79.
34. Rico CM, Majumdar S, Duarte-Gardea M, Peralta-Videa JR, Gardea-Torresdey JL. Interaction of Nanoparticles with Edible Plants and Their Possible Implications in the Food Chain. J Agric Food Chem. 2011;59:3485–98.
35. Pérez-de-Luque A. Interaction of Nanomaterials with Plants: What Do We Need for Real Applications in Agriculture? Front Environ Sci. 2017;5:12. https://doi.org/10.3389/fenvs.2017.00012.
36. Preisler AC, Guariz HR, Carvalho LB, Pereira A do ES, de Oliveira JL, Fraceto LF, et al. Phytotoxicity evaluation of poly (ε-caprolactone) nanocapsules prepared using different methods and compositions in Brassica juncea seeds. Plant Nano Biology. 2022;1:100003.
37. Yearla SR, Padmasree K. Preparation and characterisation of lignin nanoparticles: evaluation of their potential as antioxidants and UV protectants. J Exp Nanosci. 2016;11:289–302.
38. Nikolova M, Traykova B, Yankova-Tsvetkova E, Stefanova T, Dzhurmanski A, Aneva I, et al. Herbicide Potential of Selected Essential Oils From Plants of Lamiaceae and Asteraceae Families. Acta Agrobot. 2021;74.
39. Muñoz M, Torres-Pagán N, Peiró R, Guijarro R, Sánchez-Moreiras AM, Verdeguer M. Phytotoxic Effects of Three Natural Compounds: Pelargonic Acid, Carvacrol, and Cinnamic Aldehyde, against Problematic Weeds in Mediterranean Crops. Agronomy. 2020;10:791.
40. Hansen H, Hansen H. Auxin-Induced Ethylene Triggers Abscisic Acid Biosynthesis and Growth Inhibition. Plant Physiol. 2000;124:1437–48.
41. Vandenbussche F, Vaseva I, Vissenberg K, Van Der Straeten D. Ethylene in vegetative development: a tale with a riddle. New Phytol. 2012;194:895–909.
42. Zemlyanskaya EV, Omelyanchuk NA, Ubogoeva EV, Mironova VV. Deciphering Auxin-Ethylene Crosstalk at a Systems Level. Int J Mol Sci. 2018;19:4060.
43. Qin H, Huang R. Auxin Controlled by Ethylene Steers Root Development. Int J Mol Sci. 2018;19:3656.
44. Hu CH, Yuan SD, Tong CL, Zhang DJ, Huang RH. Ethylene modulates root growth and mineral nutrients levels in trifoliate orange through the auxin-signaling pathway. Not Bot Horti Agrobot Cluj Napoca. 2023;51:13269.
45. Agathokleous E, Feng Z, Peñuelas J. Chlorophyll hormesis: Are chlorophylls major components of stress biology in higher plants? Sci Total Environ. 2020;726:138637.
46. Bashri G, Prasad SM. Exogenous IAA differentially affects growth, oxidative stress and antioxidants system in Cd stressed Trigonella foenum-graecum L. seedlings: Toxicity alleviation by up-regulation of ascorbate-glutathione cycle. Ecotoxicol Environ Saf. 2016;132:329–38.
47. Hąc-Wydro K, Flasiński M. The studies on the toxicity mechanism of environmentally hazardous natural (IAA) and synthetic (NAA) auxin – The experiments on model Arabidopsis thaliana and rat liver plasma membranes. Colloids Surf B Biointerfaces. 2015;130:53–60.
48. Kraft M, Kuglitsch R, Kwiatkowski J, Frank M, Grossmann K. Indole-3-acetic acid and auxin herbicides up-regulate 9-cis-epoxycarotenoid dioxygenase gene expression and abscisic acid accumulation in cleavers (Galium aparine): interaction with ethylene. J Exp Bot. 2007;58:1497–503.
49. Grossmann K. Mode of action of auxin herbicides: a new ending to a long, drawn out story. Trends Plant Sci. 2002;5:506–8.
50. Grossmann K. Mediation of Herbicide Effects by Hormone Interactions. J Plant Growth Regul. 2003;22:109–22.
51. Xiong T, Zhang S, Kang Z, Zhang T, Li S. Dose-Dependent Physiological and Transcriptomic Responses of Lettuce (Lactuca sativa L.) to Copper Oxide Nanoparticles—Insights into the Phytotoxicity Mechanisms. Int J Mol Sci. 2021;22:3688.
52. Yan A, Chen Z. Impacts of Silver Nanoparticles on Plants: A Focus on the Phytotoxicity and Underlying Mechanism. Int J Mol Sci. 2019;20:1003.
53. Wan J, Wang R, Wang R, Ju Q, Wang Y, Xu J. Comparative Physiological and Transcriptomic Analyses Reveal the Toxic Effects of ZnO Nanoparticles on Plant Growth. Environ Sci Technol. 2019;53:4235–44.
54. Evert RF. Anatomia das plantas de Esau: meristemas,células e tecidos do corpo da planta: sua estrutura,função e desenvolvimento. 3o ed. São Paulo: Blucher; 2013.
55. Johnsson C, Jin X, Xue W, Dubreuil C, Lezhneva L, Fischer U. The plant hormone auxin directs timing of xylem development by inhibition of secondary cell wall deposition through repression of secondary wall NAC-domain transcription factors. Physiol Plant. 2019;165:673–89.
56. Yoshimoto K, Takamura H, Kadota I, Motose H, Takahashi T. Chemical control of xylem differentiation by thermospermine, xylemin and auxin. Sci Rep. 2016;6:21487.
57. Růžička K, Ursache R, Hejátko J, Helariutta Y. Xylem development – from the cradle to the grave. New Phytol. 2015;207:519–35.
58. De Zio E, Trupiano D, Karady M, Antoniadi I, Montagnoli A, Terzaghi M, et al. Tissue-specific hormone profiles from woody poplar roots under bending stress. Physiol Plant. 2019;165:101–13.

59. Kondo Y, Tamaki T, Fukuda H. Regulation of xylem cell fate. Front Plant Sci. 2014;5:315. https://doi.org/10.3389/fpls.2014.00315.
60. Pizarro A, Díaz-Sala C. Effect of polar auxin transport and gibberellins on xylem formation in pine cuttings under adventitious rooting conditions. Isr J Plant Sci. 2020;67:27–39.
61. Šípošová K, Labancová E, Hačkuličová D, Kollárová K, Vivodová Z. The changes in the maize root cell walls after exogenous application of auxin in the presence of cadmium. Environ Sci Pollut Res. 2023;30:87102–17.
62. Yuan H, Zhao L, Guo W, Yu Y, Tao L, Zhang L, et al. Exogenous Application of Phytohormones Promotes Growth and Regulates Expression of Wood Formation-Related Genes in Populus simonii × P. nigra. Int J Mol Sci. 2019;20:792.

Publisher's Note